ISSN 1674-1056
http://cpb.iphy.ac.cn
http://iopscience.iop.org/cpb
中国物理 B
Chinese Physics
中国物理 Chinese Physics B

Helicity of harmonic generation and attosecond polarization with bichromatic circularly polarized laser fields

Jun Zhang(张军), Tong Qi(齐桐), Xue-Fei Pan(潘雪飞), Jing Guo(郭静), Kai-Guang Zhu(朱凯光), Xue-Shen Liu(刘学深)
Citation: Chin. Phys. B . 2019, 28(10): 103204 . **doi:** 10.1088/1674-1056/ab4176
Journal homepage: http://cpb.iphy.ac.cn; http://iopscience.iop.org/cpb

What follows is a list of articles you may be interested in

Interpulse interference of electron emission from an atom irradiated by sinusoidally phase-modulated pulse

Hai-Ying Yuan(袁海颖), Fu-Ming Guo(郭福明), Di-Yu Zhang(张頔玉), Jun Wang(王俊), Ji-Gen Chen(陈基根), Yu-Jun Yang(杨玉军)
Chin. Phys. B . 2018, 27(10): 103201 . **doi:** 10.1088/1674-1056/27/10/103201

Simultaneous study of the lower order harmonic and photoelectron emission from an atom in intense laser pulse

Yan Yan(闫妍), Fu-Ming Guo(郭福明), Jun Wang(王俊), Ji-Gen Chen(陈基根), Yu-Jun Yang(杨玉军)
Chin. Phys. B . 2018, 27(8): 083202 . **doi:** 10.1088/1674-1056/27/8/083202

High-order harmonic generation in a two-color strong laser field with Bohmian trajectory theory

Yi-Yi Huang(黄祎祎), Xuan-Yang Lai(赖炫扬), Xiao-Jun Liu(柳晓军)
Chin. Phys. B . 2018, 27(7): 073204 . **doi:** 10.1088/1674-1056/27/7/073204

High-order harmonic generation of Li^+ with combined infrared and extreme ultraviolet fields

Li Wang(王力), Guo-Li Wang(王国利), Zhi-Hong Jiao(焦志宏), Song-Feng Zhao(赵松峰), Xiao-Xin Zhou(周效信)
Chin. Phys. B . 2018, 27(7): 073205 . **doi:** 10.1088/1674-1056/27/7/073205

Modulation of multiphoton resonant high-order harmonic spectra driven by two frequency-comb fields

Yuanyuan Zhao(赵媛媛), Di Zhao(赵迪), Chen-Wei Jiang(蒋臣威), Fu-li Li(李福利)
Chin. Phys. B . 2018, 27(5): 053202 . **doi:** 10.1088/1674-1056/27/5/053202

Helicity of harmonic generation and attosecond polarization with bichromatic circularly polarized laser fields*

Jun Zhang(张军)[1,2], Tong Qi(齐桐)[2], Xue-Fei Pan(潘雪飞)[2], Jing Guo(郭静)[2], Kai-Guang Zhu(朱凯光)[1,†], and Xue-Shen Liu(刘学深)[2,‡]

[1] College of Instrumentation and Electrical Engineering, Jilin University, Changchun 130026, China
[2] Institute of Atomic and Molecular Physics, Jilin University, Changchun 130012, China

(Received 28 June 2019; revised manuscript received 13 August 2019; published online 25 September 2019)

We theoretically investigate the high-order harmonic generation (HHG) of helium atom driven by bichromatic counter-rotating circularly polarized laser fields. By changing the intensity ratio of the two driving laser fields, the spectral chirality of the HHG can be controlled. As the intensity ratio increases, the spectral chirality will change from positive- to negative-value around a large intensity ratio of the two driving fields when the total laser intensity keeps unchanged. However, the sign of the spectral chirality can be changed from positive to negative around a small intensity ratio of the two driving fields when the total laser intensity changes. At this time, we can effectively control the helicity of the harmonic spectrum and the polarization of the resulting attosecond pulses by adjusting the intensity ratio of the two driving laser fields. As the intensity ratio and the total intensity of the driving laser fields increase, the relative intensity of either the left-circularly or right-circularly polarized harmonic can be enhanced. The attosecond pulses can evolve from being elliptical to near linear correspondingly.

Keywords: high-order harmonic generation, bichromatic circularly polarized laser fields, spectral chirality, attosecond polarization

PACS: 32.80.Rm, 42.65.Ky, 42.65.Re **DOI:** 10.1088/1674-1056/ab4176

1. Introduction

High-order harmonic generation (HHG) is a highly nonlinear phenomenon which serves as table-top sources of coherent, bright, extreme ultravilet (XUV) and soft-x-ray radiations.[1] The high harmonic can be used to generate isolated attosecond pulses and attosecond pulse trains for probing electron motion on attosecond time scale.[2] Many studies have been made to generate the supercontinuum spectrum by using linearly polarized laser fields which results in typically linearly polarized attosecond pulses. For example, a static electric field scheme,[3] the inhomogeneous laser field,[4] the chirped laser pulse,[5,6] and the two-color field[7–9] have been used to control the recolliding electron trajectory and smooth the harmonic spectrum. The HHG and isolated attosecond pulse generation in a synthesized two-color laser pulse with a wavelength-adjustable weaker pulse have also been investigated, an almost linearly polarized isolated attosecond pulse has been generated.[10] The similar coherent control of the light beams in the sum-frequency polarization beat is subtle. The polarization beat can be extended to any sum frequency of energy levels and becomes an ultra-fast process of effectively modulating attosecond pulses, which has been investigated both theoretically and experimentally.[11–13]

Circularly polarized harmonics are generated when the circularly polarized bichromatic fields interact with gas, which opens up the possibility and motivation of generating bright circularly polarized HHG.[14,15] A series of experiments investigating the ionization processes by changing the relative strength of the electric fields between the two colors in the two-color circularly polarized laser fields have been demonstrated.[16,17] Moreover, the bright circularly polarized harmonics have been generated by counterrotating circularly polarized laser fields.[14] Thus, this technique is realizable in the experiment to shape the polarization properties of the emitted attosecond pulses. The circularly polarized (CP) HHG of the ellipticity from linear to almost circular can be generated driven by bichromatic counter-rotating circularly polarized (BCCP) laser fields. Recently, the circularly-polarized light and the non-linearly polarized attosecond pulse have been a hot topic due to their applications of probing chiral-specific phenomena, such as ultrafast spin dynamics[14] and magnetic circular dichroism.[15]

The BCCP laser field consists of a circularly polarized fundamental field and its counter-rotating second harmonic, which results that the total field has the three-fold symmetry.[18] According to the angular momentum selection rules, only the harmonics orders $3N+1$ and $3N+2$ are al-

*Project supported by the National Natural Science Foundation of China (Grant No. 61575077), the Natural Science Foundation of Jilin Province of China (Grant No. 20180101225JC), the China Postdoctoral Science Foundation (Grants Nos. 2018M641766 and 2019T120232), and the Graduate Innovation Fund of Jilin University, China (Grant No. 101832018C105).

†Corresponding author. E-mail: zhukaiguang@jlu.edu.cn
‡Corresponding author. E-mail: liuxs@jlu.edu.cn

© 2019 Chinese Physical Society and IOP Publishing Ltd

lowed, while the $3N$ harmonics are forbidden in a BCCP laser field. Most recently, the control of the helicity of circularly polarized high harmonics has been achieved by changing the intensities of the two fields, and the elliptically polarized attosecond pulse trains (APTs) have been generated.[19,20] In the same respect, the time delay between the bichromatic laser fields can be adjusted to control either the right- or left-circularly polarized harmonics.[21] The generation of circularly polarized high-order harmonics has been investigated by controlling the electron recollisions, a classical trajectory analysis and quantum studies have been presented.[22] A scheme to generate tunable chirality of APTs from nearly linear to nearly circular has been illustrated by using the BCCP laser field, the results show that the ellipticity of the APTs is sensitive to the relative phase of the BCCP laser field.[23]

In this paper, we investigate the high harmonics generated in the two-dimensional (2D) helium atom model by the BCCP laser fields. The chirality of high harmonics and ellipticity of the APTs are illustrated by changing the intensity ratio of the two driving laser fields with different total intensities, and the ellipticity of the APTs can be varied correspondingly.

2. Theoretical model

We investigate the HHG and attosecond pulse from helium atom interacting with a BCCP laser field based on the single-electron approximation. The harmonic spectrum generation can be investigated by numerically solving the two-dimensional time dependent Schrödinger equation (2D-TDSE) using the second-order splitting-operator fast Fourier transform algorithm.[24] The initial wave function is constructed by the imaginary time-propagation method. The 2D-TDSE reads (in atomic units)

$$\mathrm{i}\frac{\partial\psi(x,y,t)}{\partial t}=\left[\frac{P_x^2+P_y^2}{2}+V(x,y)+xE_x(t)+yE_y(t)\right]\psi(x,y,t), \tag{1}$$

where $V(x,y)=-1/\sqrt{x^2+y^2+a^2}$ is the soft-core Coulomb potential. We choose soft-core parameter $a=0.2619$ so that the energy eigenvalue of ground state is 0.904 a.u., which is equal to the first ionization energy of the helium atom.[25,26] The length of the integration grid is 409.6 a.u. with the spatial step 0.4 a.u. and the time step 0.1 a.u.

The dipole acceleration can be given according to the Ehrenfest theorem[27,28]

$$\begin{aligned}\boldsymbol{a}(t) &= \langle\psi(x,y,t)|-\boldsymbol{\nabla}(x,y)-\boldsymbol{E}(t)|\psi(x,y,t)\rangle\\ &= \langle\psi(x,y,t)|\,\boldsymbol{e}_x\left[-\frac{\partial V(x,y)}{\partial x}-E_x(t)\right]\\ &\quad+\boldsymbol{e}_y\left[-\frac{\partial V(x,y)}{\partial y}-E_y(t)\right]|\psi(x,y,t)\rangle\\ &= a_x(t)\,\boldsymbol{e}_x+a_y(t)\,\boldsymbol{e}_y.\end{aligned} \tag{2}$$

The HHG spectrum can be obtained by means of Fourier transformation of $\boldsymbol{a}(t)$

$$\begin{aligned}P(\omega) &\sim \left|\frac{1}{T}\int_0^T[a_x(t)\boldsymbol{e}_x+a_y(t)\boldsymbol{e}_y]\,\mathrm{e}^{-\mathrm{i}\omega t}\,\mathrm{d}t\right|^2\\ &= |a_x(\omega)\boldsymbol{e}_x|^2+|a_y(\omega)\boldsymbol{e}_y|^2.\end{aligned} \tag{3}$$

The harmonic intensity of the left- and right-polarized harmonic components can be obtained by

$$D_\pm(\omega)=|a_\pm(\omega)|^2, \tag{4}$$

where $a_\pm(\omega)=\frac{1}{\sqrt{2}}(a_x(\omega)\pm\mathrm{i}a_y(\omega))$.

The temporal profile of an attosecond pulse can be obtained by superposing several harmonics

$$I_x(t)=|a_{xq}(t)\,\mathrm{e}^{\mathrm{i}q\omega t}|^2, \tag{5}$$

$$I_y(t)=|a_{yq}(t)\,\mathrm{e}^{\mathrm{i}q\omega t}|^2. \tag{6}$$

3. Results and discussion

We investigate the helicity of harmonic generation from helium atom in a BCCP laser field. The BCCP laser field in the (x, y) polarization plane is given as[29,30]

$$\begin{aligned}\boldsymbol{E}(t) &= \frac{E_0}{1+\gamma_E}f(t)[\cos(\omega t)\hat{\boldsymbol{x}}+\sin(\omega t)\hat{\boldsymbol{y}}]\\ &\quad+\frac{\gamma_E E_0}{1+\gamma_E}f(t)[\cos(2\omega t)\hat{\boldsymbol{x}}-\sin(2\omega t)\hat{\boldsymbol{y}}],\end{aligned} \tag{7}$$

where E_0 is the amplitude of the laser pulse, γ_E is the intensity ratio, and $\omega=0.05$ a.u. is the frequency of the laser pulse. It is illustrated that the total intensity of the BCCP laser field expressed in Eq. (7) keeps unchanged for different intensity ratios. The envelope of the laser pulse $f(t)$ is a 9-optical-cycle trapezoidal pulse with 2-cycle ramp on, 5-cycle constant, and 2-cycle ramp off.

The spectral chirality can be characterized by the degree of chiral $\chi=\frac{I_{\mathrm{LCP}}-I_{\mathrm{RCP}}}{I_{\mathrm{LCP}}+I_{\mathrm{RCP}}}$, where I_{LCP} and I_{RCP} are the total integrated signals of the left-circularly polarized (LCP) and right-circularly polarized (RCP) harmonics for all orders of the harmonic spectra, respectively. In Fig. 1(a), we present the theoretical spectral chirality in helium atom by the BCCP laser field with different intensity ratios at the total intensities of $E_0=0.05$ a.u. and 0.1 a.u., respectively. From Fig. 1(a), we can see that the spectral chirality on HHG can be controlled by adjusting the intensity ratio γ_E. As the intensity ratio increases, the spectral chiral changes from positive- to negative-value when the intensity ratio γ_E equals to 8 and 6 for $E_0=0.05$ a.u. and 0.1 a.u., respectively. It is easier to change the sign of the spectral chirality for $E_0=0.1$ a.u. than the $E_0=0.05$ a.u. case. The generation of harmonic spectrum can be explained by the three steps of ionization, acceleration, and recombination. The relation between the tunneling ionization rates and the laser intensity is highly nonlinear so that

the ionization rates are sensitive to the intensity ratios of the two components of the bicircular field.[31] As the intensity ratio of the BCCP laser field is altered, the process of HHG and the corresponding spectral intensities of the LCP or RCP harmonic are altered as well, which results in different spectral chiralities.

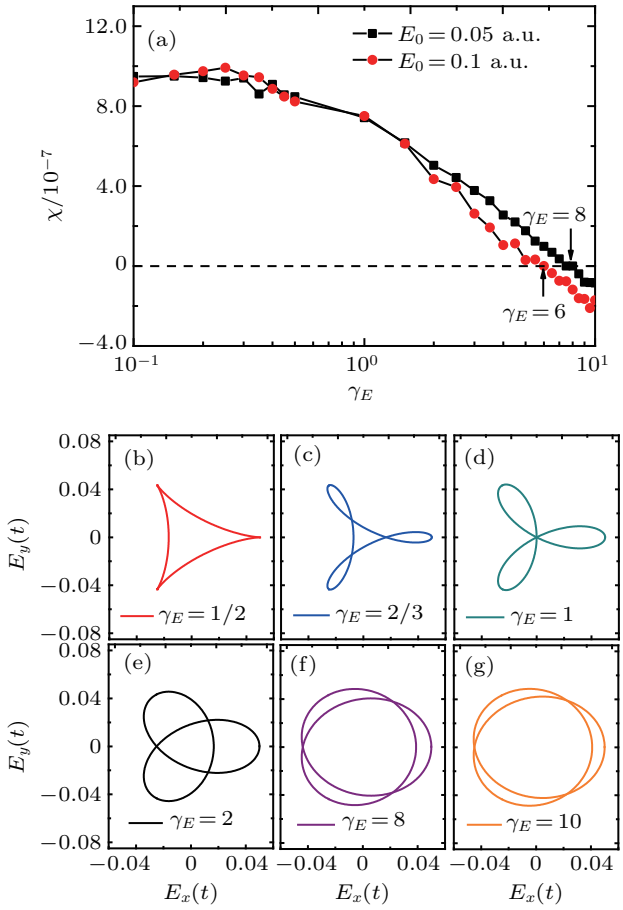


Fig. 1. (a) Spectral chirality $\chi = \frac{I_{\rm LCP} - I_{\rm RCP}}{I_{\rm LCP} + I_{\rm RCP}}$ as a function of the intensity ratio γ_E in BCCP laser fields with the same total intensities $E_0 = 0.05$ a.u. and 0.1 a.u. Lissajous diagrams of BCCP laser fields with different intensity ratios: (b) $\gamma_E = 1/2$, (c) $\gamma_E = 2/3$, (d) $\gamma_E = 1.0$, (e) $\gamma_E = 2.0$, (f) $\gamma_E = 8.0$, (g) $\gamma_E = 10.0$.

To further understand the underlying physical mechanisms, we will give a qualitative explanation. The HHG spectrum driven by a bichromatic circularly polarized laser field shows that only the harmonic orders $3N+1$ (left circularly polarized harmonic) and $3N+2$ (right circularly polarized harmonic) are allowed, while the $3N$ harmonic orders are forbidden. The $3N+1$ order is generated by absorbing $(N+1)\omega$ photons and $(N)2\omega$ photons, i.e., one extra photon from the ω field. The $3N+2$ order is generated by absorbing $(N+1)2\omega$ photons and $(N)\omega$ photons, i.e., one extra photon from the 2ω field. As the intensity ratio increases, the right circularly polarized HHG ($3N+2$ order) is enhanced by absorbing the extra photon from the 2ω field. Thus, the spectral chirality of the HHG will change from positive to negative-value as shown in Fig. 1(a).

The Lissajous figures of the BCCP laser fields with different intensity ratios ($\gamma_E = 1/2$, 2/3, 1.0, 2.0, 8.0, 10.0) are demonstrated in Figs. 1(b)–1(g), respectively. For the intensity ratio $\gamma_E = 1.0$, the counter-rotating circularly polarized laser fields reflect a three-lobed type. For the intensity ratio $\gamma_E < 1.0$ (such as $\gamma_E = 1/2,\ 2/3$), the three lobes structure gradually becomes inconspicuous until it becomes approximately an equilateral triangle. For the intensity ratio $\gamma_E > 1.0$ (such as $\gamma_E = 2.0,\ 8.0,\ 10.0$), the width of the three-lobed structure is significantly widened until it is close to circularly polarized. From Fig. 1(a), we can see that the chirality control of the HHG spectrum can be achieved with a larger intensity ratio γ_E ($\gamma_E = 8,\ 6$) of the BCCP laser field, but it will lead to a suppression of harmonic emission by such an approximate circularly polarized laser field.[32] How to change the sign of the spectral chiral without affecting the HHG efficiency is the research focus of this paper.

In order to control the spectral chirality effectively, we reconsider the laser field in the (x, y) polarization plane as

$$\begin{aligned} \boldsymbol{E}'(t) \;=\; & E_1 f(t)[\cos(\omega t)\hat{\boldsymbol{x}} + \sin(\omega t)\hat{\boldsymbol{y}}] \\ & + \gamma_E' E_1 f(t)[\cos(2\omega t)\hat{\boldsymbol{x}} - \sin(2\omega t)\hat{\boldsymbol{y}}], \end{aligned} \tag{8}$$

where $E_1 = 0.05$ a.u. is the amplitude of the laser pulse. The total intensity of the BCCP laser field is dependent on the intensity ratio γ_E' and the other laser parameters are the same as those given under Eq. (7).

Figure 2 presents the theoretical spectral chirality in helium atom by the BCCP laser field across a range of intensity ratios and total intensities. From Fig. 2, we can see that the spectral chirality on HHG is more sensitive to the intensity ratios than the case in Fig. 1(a) due to the change of the total laser intensities. We observe that the sign of the spectral chirality is not changed and the LCP spectrum keeps the dominant role for the intensity ratios $\gamma_E' < 1.0$. For the intensity ratios $1.25 < \gamma_E' < 2.0$, the spectral chirality decreases with the increase of the intensity ratio and the sign of the spectral chirality changes from positive to negative. The corresponding helicity of harmonics changes from LCP to RCP. For the intensity ratios $2.0 < \gamma_E' < 3.0$, the spectral chirality increases with the increase of the intensity ratio and the sign of the spectral chirality changes from negative to positive. The corresponding helicity of harmonics changes from RCP to LCP again. And then it decreases and increases with the increase of the intensity ratio back and forth until $\gamma_E' = 10.0$. The spectral chirality shows two almost equal negative intensity peaks, which means that the RCP harmonics dominate for the intensity ratios $\gamma_E' = 2.0$ and $\gamma_E' = 7.0$. These results indicate that the spectral chirality can be effectively controlled by the intensity ratio over a range of total intensities of the driving field.

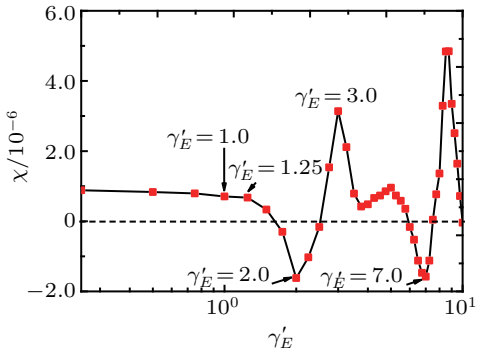


Fig. 2. Spectral chirality as a function of the intensity ratio γ'_E in BCCP laser fields for $E_1 = 0.05$ a.u. with different total laser intensities.

The physical explanation to that the spectral chirality of the HHG changes with the parameters of the bichromatic laser fields for the same total intensity as shown in Fig. 1(a) has be given qualitatively above. However, the physical mechanism with changing the total intensity as shown in Fig. 2 is more complicated, we will try to give the qualitative explanations. From Fig. 1(a), we can see that the sign of the spectral chirality changes from positive to negative when the intensity ratio γ_E equals to 8 for $E_0 = 0.05$ a.u. In this case, the amplitude difference between the left and right circularly polarized laser pulses is $E_0 \times (\gamma_E - 1)/(\gamma_E + 1) = 0.05 \times 7/9$ a.u. $= 0.039$ a.u. From Fig. 2, we can see that the sign of the spectral chirality changes from positive to negative when the intensity ratio γ'_E equals to 1.63 with changing total intensity for $E_1 = 0.05$ a.u. The amplitude difference between the left and right circularly polarized laser pulses is $E_1 \times (\gamma'_E - 1) = 0.05 \times 0.63$ a.u. $= 0.0315$ a.u., which is close to the amplitude difference 0.039 a.u. illustrated in Fig. 1(a). Therefore, the sign of the spectral chirality can be changed with a smaller intensity ratio (i.e., $\gamma'_E = 1.63$ as shown in Fig. 2, where $\gamma'_E = 2$ is located in the negative intensity peak of the spectral chirality).

Due to the sign of the spectral chirality is more sensitive to the intensity ratios by the change of the total intensity compared with the case by the same total intensity, we will take $\gamma'_E = 1.0$ and $\gamma'_E = 2.0$ (which corresponds to a negative peak of spectral chirality) as examples to investigate the high harmonics and ellipticity of the APTs.

Figure 3 shows the harmonic spectra of the left- (red lines) and right-circularly (blue lines) polarized harmonics generated from helium atom with the intensity ratios $\gamma'_E = 1.0$ and $\gamma'_E = 2.0$, respectively. The spectra present the general harmonic structure in a BCCP laser field where the harmonics appear in pairs with alternating helicity and the $3N\omega$ harmonics are suppressed. The ratios of the adjacent $3N+1$ and $3N+2$ harmonic intensities are labeled with red and blue numbers, respectively. When the ratios are larger (red numbers) or smaller (blue numbers) than 1.0, the LCP or the RCP harmonic spectra dominate.

Figure 3(a) shows the harmonic spectrum with $\gamma'_E = 1.0$, the result shows that the harmonic spectrum has alternating helicity before 34th order and the intensities of the LCP harmonics are higher than those of the RCP harmonics near the harmonic cutoff. Figure 3(b) shows the harmonic spectrum with $\gamma'_E = 2.0$, it indicates that the cutoff of the harmonic spectrum is extended compared with the case in Fig. 3(a). The harmonic spectrum shown in Fig. 3(b) can be divided into three parts according to the helicity. The first part is before 28th harmonic order, the intensities of the RCP harmonics are higher than those of the LCP harmonics. The second part is between 34th and 55th order, the intensities of the LCP harmonics are higher than those of the RCP harmonics. The third part is near the harmonic cutoff, the intensities of the RCP harmonics are higher than those of the LCP harmonics. The overall harmonic helicities are dependent on the intensity ratio and the total intensities affect the cutoff of the harmonic spectrum as demonstrated in Ref. [19]. Thus, both the harmonic helicities and the harmonic cutoff are changed when the intensity ratio is increased to $\gamma'_E = 2.0$ compared with the $\gamma'_E = 1.0$ case.

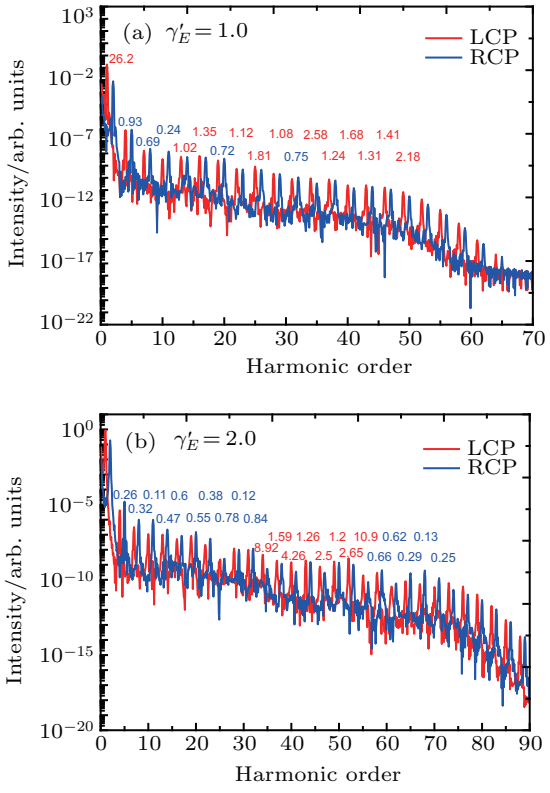


Fig. 3. High-order harmonic spectra of helium atom with the intensity ratio (a) $\gamma'_E = 1.0$ and (b) $\gamma'_E = 2.0$. The other laser parameters are the same as those in Fig. 2. The intensity ratios of the adjacent harmonic orders (H_{3N+1}/H_{3N+2}) are labeled with red and blue numbers, respectively.

Next, we illustrate the attosecond pulse trains with dif-

ferent ellipticities obtained from our scheme with different intensity ratios as indicated in Fig. 3. Figure 4 shows the APTs synthesized by superposing a series of high harmonics for the cases of $\gamma'_E = 1.0$ and $\gamma'_E = 2.0$, respectively. By superposing harmonics from 30th to 40th order for the case of $\gamma'_E = 1.0$, which corresponds to the helicity alternating of harmonics, the elliptically polarized APTs are generated as shown in Fig. 4(a). By superposing harmonics from 40th to 50th order for the case of $\gamma'_E = 1.0$, which corresponds to the LCP harmonics, the linearly polarized APTs are generated, as shown in Fig. 4(b). As the harmonic orders are increased, an increase in the relative intensity of the LCP harmonics is induced. The polarization of the attosecond bursts evolves from elliptical [Fig. 4(a)] to near linear [Fig. 4(b)]. Figure 4(c) presents the APTs by superposing the harmonics from 30th to 40th order for the case of $\gamma'_E = 2.0$, which corresponds to the LCP harmonics. Figure 4(d) presents the APTs by superposing the harmonics from 40th to 50th order for the case of $\gamma'_E = 2.0$, which corresponds to the RCP harmonics. The linearly polarized APTs are generated for both cases as shown in Figs. 4(c) and 4(d).

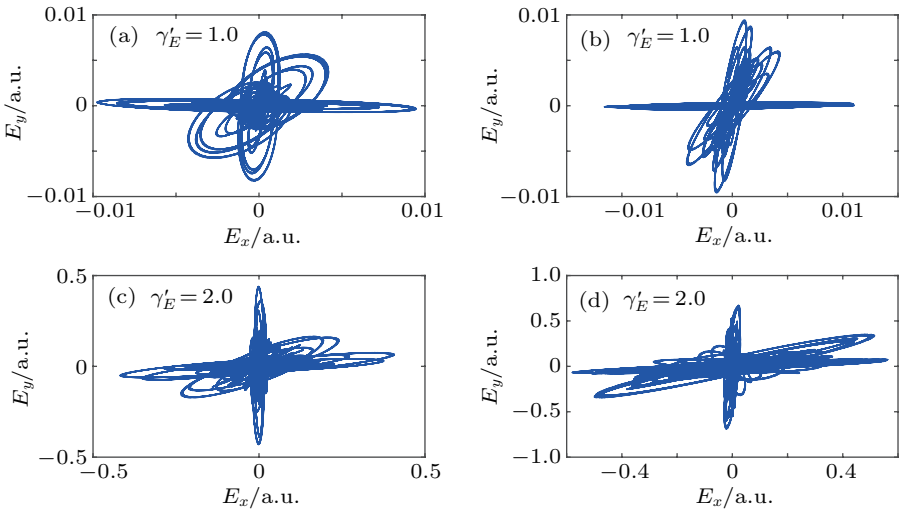


Fig. 4. Attosecond pulse trains with the intensity ratios $\gamma'_E = 1.0$ generated by superposing the harmonics (a) from 30th to 40th order and (b) from 40th to 50th order. Attosecond pulse trains with the intensity ratios $\gamma'_E = 2.0$ generated by superposing the harmonics (c) from 37th to 47th order and (d) from 60th to 70th order. The other laser parameters are the same as those in Fig. 2.

4. Conclusion

We have theoretically investigated the helicity of harmonic generation and the attsecond pulse polarization by solving the two-dimensional time dependent Schrödinger equation. The results show that the spectral chirality of high harmonics decreases slowly with the increase of the intensity ratio between the two driving fields at the same total intensity. The spectral chirality of high harmonics will change from positive- to negative-value with a large intensity ratio. We also investigate the control of the spectral chirality by adjusting the intensity ratio accompanied by the change of the total intensity. The sign of the spectral chirality can be changed at a small intensity ratio. At this time, either the right circularly polarized harmonic or the left circularly polarized harmonic is selectively enhanced. The elliptical and near linear attosecond pulse trains have been synthesized by superposing the proper harmonics.

References

[1] Rundquist A, Durfee C G, Chang Z, Herne C, Backus S, Murnane M M and Kapteyn H C 1998 *Science* **280** 1412
[2] Krausz F and Ivanov M 2009 *Rev. Mod. Phys.* **81** 163
[3] Miao X Y and Zhang C P 2014 *Laser Phys. Lett.* **11** 115301
[4] Ge X L, Du H, Wang Q, Guo J and Liu X S 2015 *Chin. Phys. B* **24** 023201
[5] Li P C, Zhou X X, Wang G L and Zhao Z X 2009 *Phys. Rev. A* **80** 053825
[6] Zhang J, Du H, Liu H F, Guo J and Liu X S 2016 *Opt. Commun.* **366** 457
[7] Feng L Q and Liu H 2015 *Chin. Phys. B* **24** 034206
[8] Zhang H D, Guo J, Shi Y, Du H, Liu H F, Huang X R, Liu X S and Jing J 2017 *Chin. Phys. Lett.* **34** 014206
[9] Zhang K, Liu M, Wang B B, Guo Y C, Yan Z C, Chen J and Liu X J 2017 *Chin. Phys. Lett.* **34** 113201
[10] Xia C L, Ge X L, Zhao X, Guo J and Liu X S 2012 *Phys. Rev. A* **85** 025802
[11] Zhang Y, Gan C, Song J, Yu X, Ma R, Ge H, Li C and Lu K 2005 *Phys. Rev. A* **71** 023802
[12] Zhang Y, de Araújo C B and Eyler E E 2001 *Phys. Rev. A* **63** 043802
[13] Du Y, Zhang Y, Zuo C, Li C, Nie Z, Zheng H, Shi M, Wang R, Song J, Lu K and Xiao M 2009 *Phys. Rev. A* **79** 063839
[14] Fan T, Grychtol P, Knut R, Hernández-García C, Hickstein D D, Zusin D, Gentry C, Dollar F J, Mancuso C A, Hogle CW, Kfir O, Legut D, Carva K, Ellis J L, Dorney K M, Chen C, Shpyrko O G, Fullerton E E, Cohen O, Oppeneer P M, Milošević D B, Becker A, Jaroń-Becker A A, Popmintchev T, Murnane M M and Kapteyn H C 2015 *Proc. Natl. Acad. Sci. USA* **112** 14206
[15] La-O-Vorakiat C, Siemens M, Murnane M M and Kapteyn H C 2009 *Phys. Rev. Lett.* **103** 257402
[16] Mancuso C A, Dorney K M, Hickstein D D, Chaloupka J L, Ellis J L, Dollar F J, Knut R, Grychtol P, Zusin D, Gentry C, Gopalakrishnan M, Kapteyn H C and Murnane M M 2016 *Phys. Rev. Lett.* **117** 133201
[17] Eckart S, Richter M, Kunitski M, Hartung A, Rist J, Henrichs K, Schlott N, Kang H, Bauer T, Sann H, Schmidt L Ph H, Schöffler M, Jahnke T and Dörner R 2016 *Phys. Rev. Lett.* **117** 133202

[18] Bandrauk A D, Mauger F and Yuan K J 2016 *J. Phys. B: At. Mol. Opt. Phys.* **49** 23LT01
[19] Dorney K M, Ellis J L, Hernández-García C, Hickstein D D, Mancuso C A, Brooks N, Fan T, Fan G, Zusin D, Gentry C, Grychtol P, Kapteyn H C and Murnane M M 2017 *Phys. Rev. Lett.* **119** 063201
[20] Jimeńez-Galań A, Zhavoronkov N, Ayuso D, Morales F, Patchkovskii S, Schloz M, Pisanty E, Smirnova O and Ivanov M 2018 *Phys. Rev. A* **97** 023409
[21] Jimeńez-Galań A, Zhavoronkov N, Schloz M, Morales F and Ivanov M 2017 *Opt. Express* **25** 22880
[22] Heslar J, Telnov D A and Chu S I 2018 *Phys. Rev. A* **97** 043419
[23] Zhang X, Zhu X, Liu X, Wang D, Zhang Q, Lan P and Lu P 2017 *Opt. Lett.* **42** 1027
[24] Feit M D and Fleck J A 1983 *Jr, J. Chem. Phys.* **78** 301
[25] Moler C and Loan C V 2003 *SIAM Rev.* **45** 3
[26] Dixit G, Jimeńez-Galań Á, Medisăauskas L and Ivanov M 2018 *Phys. Rev. A* **98** 053402
[27] Bian X B and Bandrauk A D 2010 *Phys. Rev. Lett.* **105** 093903
[28] Burnett K, Reed V C, Cooper J and Knight P L 1992 *Phys. Rev. A* **45** 3347
[29] Zhang J, Qi T, Zhu K G and Liu X S 2019 *Laser Phys.* **29** 105301
[30] Zhang X, Li L, Zhu X, Liu X, Zhang Q, Lan P and Lu P 2016 *Phys. Rev. A* **94** 053408
[31] Milošević D B and Becker W 2016 *Phys. Rev. A* **93** 063418
[32] Yuan K J and Bandrauk A D 2011 *Phys. Rev. A* **83** 063422